Silica and core-shell nanospheres by supercritical fluid assisted sol-gel synthesis

N. Murillo-Cremaes, E. Taboada, C. Domingo, A. Roig*
Institut de Ciència de Materials de Barcelona (ICMAB-CSIC), Campus de la UAB, 08193 Bellaterra, Spain. e-mail: roig@icmab.es

ABSTRACT

Fabrication of monodisperse pure silica and core-shell nanospheres (Fe_2O_3@SiO_2 and Fe_2O_3/QD@SiO_2) was done in straight forward one-pot method combining sol-gel chemistry and supercritical fluids. For the core-shell materials, preformed nanoparticles stabilized in hexane were dispersed in a sol containing a silicon alkoxide, water and acetone as the solvent. The precursor solution was introduced in an autoclave and pressurized with compressed CO_2. Then, pressure and temperature were raised over the supercritical conditions of the CO_2/acetone mixture allowing the silicon alkoxide to hydrolyze and condensate forming the silica shell. The composite gel nanospheres got dried as the solvent was extracted at supercritical conditions. They present a narrow particle size distribution (with less than 30% polidispersity). Each nanosphere consists of a functional core of several non-contacting γ-Fe_2O_3 nanoparticles and/or quantum dots surrounded by a microporous silica shell. Their size can be tuned by controlling the reaction conditions. The same synthetic approach is followed to fabricate microporous pure silica nanoparticles. Advantages of the method are short reaction times compared to non-supercritical sol-gel procedures, high reaction yield and purity of the product. In addition, the method has potentiality to be scaled up.

Key words: magnetic, silica, core-shell, nanoparticles, aerogels.

INTRODUCTION

Silica-based particles are of interest in different industrial sectors; they have been reported in applications as additives for conventional foaming operations, chromatography packing materials, controlled release drug nanocarriers and high surface-area adsorbents, among others. [1, 2] Sol-gel method from metal alkoxides and the use of structure directing agents have been widely used for the synthesis of ordered mesoporous silica materials. [3, 4] Synthesis of nanoparticles in conventional solvents is often a multi-step process that needs long processing times, often requiring intermediate separation or purification steps (very important when targeting biomedical applications) that not only reduce the net material yield but seriously impede the up-scaling of the material's production. In addition, liquid media transmits temperature or composition changes slowly which may result in a poor control over the particle size. Besides a drying alternative, supercritical fluids are more and more used as a reaction media to produce new particulate complex materials. [5, 6] Production of silica particles combining sol-gel chemistry and supercritical fluids should provide among other advantages the reduction of synthetic steps compared to other sol-gel processing approaches. Scheme 1 summarizes the versatility of sol-gel synthesis together with supercritical fluids to obtain silica materials including the porous silica particles.

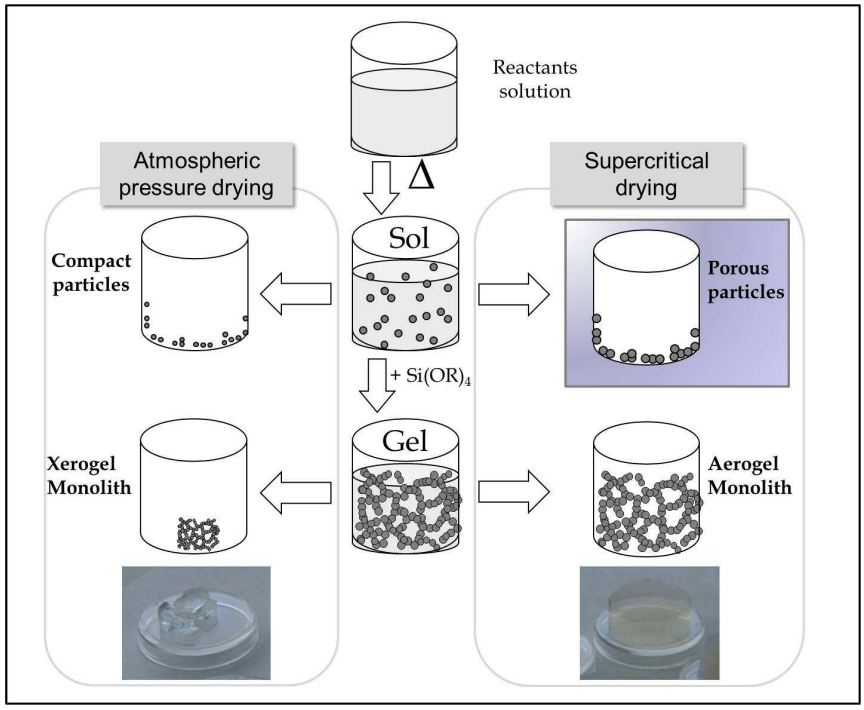

Scheme 1. Sol-gel method combined with supercritical fluids for producing silica materials, including porous silica particles.

Silica sol-gel reactions have previously been directly performed in supercritical carbon dioxide as a reactive medium by using formic acid as condensation agent. [7] Here, we report on the fabrication of monodisperse microporous silica and core-shell nanospheres in straight forward one-pot method combining sol-gel chemistry and supercritical fluids. Our approach found inspiration in a classic aerogel synthesis and mainly deals with the dissolution of precursors in supercritical fluids, followed by the hydrolysis and condensation reactions and drying under supercritical conditions. [8-10] The as-obtained core-shell nanospheres consist of a functional core of several non-contacting γ-Fe_2O_3 nanoparticles and/or quantum dots surrounded by a microporous silica shell. Their size can be tuned by controlling the reaction conditions. The synthetic route presented here has several important advantages over previously described ones since it allows the control over the particle size, narrow particle size distribution without a particle size separation step are obtained, relatively fast processing time, high material yield and microporosity without the use of catalyst or structure inducing agents. In addition, the nanospheres can be easily stabilized as an aqueous colloidal dispersion and the method has potentiality to be scaled up. Biomedical applications: drug delivery vehicles, contrast agents for magnetic resonance imaging and optical sensors are the target applications for these systems. Results on applicability are out of the scope of this study and have been reported somewhere else. [10, 11]

.

MATERIALS AND METHODS

Synthesis

For the core-shell nanospheres, maghemite nanoparticles (γ-Fe_2O_3-NPs) were pre-synthesized by a modification of the method firstly described by Hyeon et al. [12] In a typical experiment, the resulting particles are 6 nm of mean diameter, with very narrow particle size

distribution (typically < 10%) and they remain stable in hexane for months. Nanoparticles are superparamagnetic at room temperature. Quantum dots (CdSe)SPb were kindly donated by Can GmbH (Germay) and the particles have a mean size of 6 nm and are stabilized in hexane. Coating of the functional nanoparticles with silica is done combining sol-gel hydrolysis and condensation of a silicon precursor and supercritical evacuation of the solvent inside an autoclave. Typically, initial reagents with a mass composition TMOS/H_2O/acetone/Fe_2O_3 or QD/hexane 0.92/0.22/95.63/0.04/3.19 wt. % were placed in a Pyrex vessel at ambient conditions; the TMOS/H_2O molar ratio was kept fixed at 0.5 and the acetone/hexane volume ratio at 70. Nor catalysts, surfactants or any other pore inducers were used. The vessel was then introduced in the 2 litres supercritical reactor and the pressure inside the reactor was increased up to 50 bar using carbon dioxide (CO_2). Afterwards, temperature was raised up to 250ºC with the corresponding increase of pressure up to 250 bar. The final P and T values are over the critical point of any possible CO_2/acetone solvent mixture (P_c (max) = 120 bar and T_c (max) = 235ºC). After a given residence time at supercritical conditions, the system was depressurized up to 150 bar (still supercritical conditions) and fresh CO_2 was circulated for one hour with a flow of 0.5 kg_{CO2}/h and another hour at 1.5 kg_{CO2}/h. The circulation of clean CO_2 serves to drag out of the vessel the unreacted silicon precursor and thus, minimize the necking formation between the particles. Finally, the autoclave was depressurized and cooled down to room temperature. The resulting material is a dry powder and it is homogeneously distributed around the reactor walls. Several batches of pure silica nanoparticles have been fabricated following the same approach. Each experiment took eight hours. In view of the use of these materials for biomedical applications, methanol was avoided because of its higher toxicity (although it is the most appropriate alcohol to dissolve TMOS) and acetone was used instead.

Characterization techniques

Transmission electron microscopy (TEM): a JEOL JEM-1400 microscope operating at 200 keV was used to observe the materials. *Scanning electron microscopy (SEM)*: Philips SEM 515 microscope operating at 0.2-30 kV, equipped with secondary and backscattering electrons detectors. *Dynamic Light Scattering (DLS) and Zeta Potential (ζ)* were performed with a Zetasizer Nano ZS (Malvern Instruments), provided with a He/Ne laser of 633 nm wavelength. *BET*: Nitrogen adsorption data were taken at 77 K using an ASAP 2000 surface area analyzer (Micromeritics Instrument Corporation) after degasification under vacuum for 24 h to remove the adsorbed species. Surface area and mean pore diameter determinations were carried out following BET (Brunauer, Emmett and Teller) and BJH (Barrett, Joyner and Halenda) models, respectively. *Chemical analysis:* The elemental composition was measured by inductively coupled-plasma mass spectroscopy (ICP-MS). *XRD*. The core-shell samples were characterized by X-ray diffraction with a Siemens D5000 X-ray powder diffractometer using Cu Kα incident radiation. Crystallite size determination was done by applying the Scherrer's formula to the 400, 511 and 440 peaks. *Magnetic Measurements*: Magnetization vs. applied magnetic field at 5 K and 298 K and the zero-field cooling-field cooling (ZFC-FC) curves with a 100 Oe applied field were measured with a superconducting quantum interference device (SQUID) magnetometer (Quantum Design MPMS5XL). All the magnetization data are presented in units of (Am^2)/kg γ-Fe_2O_3, SI units (equivalent to emu/g Fe_2O_3, cgs units).

RESULTS

The selected set of materials to be presented here are two samples of pure silica nanospheres with different sizes (SiO_2[1] and SiO_2[2]) with 200 and 2000 nm respectively and two core-shell systems, one with magnetic nuclei (Fe_2O_3@SiO_2) and one with quantum dots and magnetic nuclei (Fe_2O_3/QD)@SiO_2) (in this later system, the initial nanocrystals distribution was of 61 % of iron oxide leaving a 39% of quantum dots). Table 1 contains some reaction parameters and physico-chemical characteristics of the selected materials.

Sol-gel route to silica materials can make use of alkoxydes. The most commonly ones are tetramethoxy silane (TMOS; $Si(OCH_3)_4$) and tetraethoxysilane (TEOS; $Si(OCH_2CH_3)_4$), which are colourless liquids and insoluble in water. Therefore, a common solvent is often needed to dissolve both reactants. Methanol and ethanol are usually the selected solvents for TMOS and TEOS, respectively. It is advisable to combine the silicon precursor and the solvent with the same organic radical (R = methyl or ethyl group) in order to avoid transesterification reactions which may create inhomogeneities in the gel due to the different kinetics of each organic radical. Other solvents with no alkoxy groups and therefore unable to perform transesterification reactions are also appropriate, provided that they dissolve the reactants; for example, acetone. Acid or basic catalysts can be used to accelerate the reaction and modify the mechanism, inducing changes in the structure and properties of the resulting materials. Thus, the parameters influencing the hydrolysis and condensation reactions, and consequently, the properties of the final material are numerous. Among them, are the type of precursor, precursor to water ratio, type of catalyst, type of solvent, temperature, pH and the relative and absolute concentration of the components in the precursor mixtures. [13] For the materials selected, the common parameters in all synthesis were: the use of TMOS and acetone (500 ml), a molar ratio of TMOS: H_2O of 0.5 and no addition of catalyst.

Table 1. Experimental parameters for selected materials in supercritical media. Main results on the synthesis of pure silica aerogel particles. *Size values from SEM observations, size polydispersity (P) is included within parenthesis.

Synthesis ID	$[Si(OR)_4]$ (M)	Residence time (min)	Mass Yield (%)	Size (nm)* (P)	Surface area (m^2/g)	Core size (nm)
SiO_2[1]	0.15	5	64	204 (5%)	307	-
SiO_2[2]	0.05	120	64	2400 (30%)	183	-
Fe_2O_3@SiO_2	0.05	120	73	65 (19%)	160	24 (33%)
(Fe_2O_3/QD)@SiO_2	0.05	120	62	156 (19%)	-	50 (29%)

The resulting materials were very light-weighted in the form of a dry powder, white -for silica particles- or brown -in case of the core-shell ones-. The powder was dispersed all over the autoclave both inside and outside the Pyrex vessel (see Figure 1). [14]

Figure 1. Photographs of the supercritical reactor (left image) and the Pyrex vessel (with glass wool cover; middle image) just after an experiment of pure silica particles. The collected powder can be seen in the lower part of the middle image. A typical batch yielded 2 grams of material. Right upper image presents a schematic view of the magnetic responsive core-shell nanospheres which are also shown in the lower panel.

Particle size and shape was analyzed with scanning and transmission electron microscopies (SEM and TEM). It is very important not to disperse the silica particles in water for TEM observation to avoid further silica hydrolysis and condensation when the material is exposed to the high energy beam of the microscope. For that reason acetone is preferred. The materials were composed of spherical particles with no necking between them. Their size ranged from 2 microns to 200 nm in diameter depending mainly on the residence time: longer residence time produced larger particles. Particle size distributions of pure silica spheres as low as 5% were obtained without the need of any size selection process, as shown in Figure 2, while size distributions of core@shell particles are displayed in Figure 3.

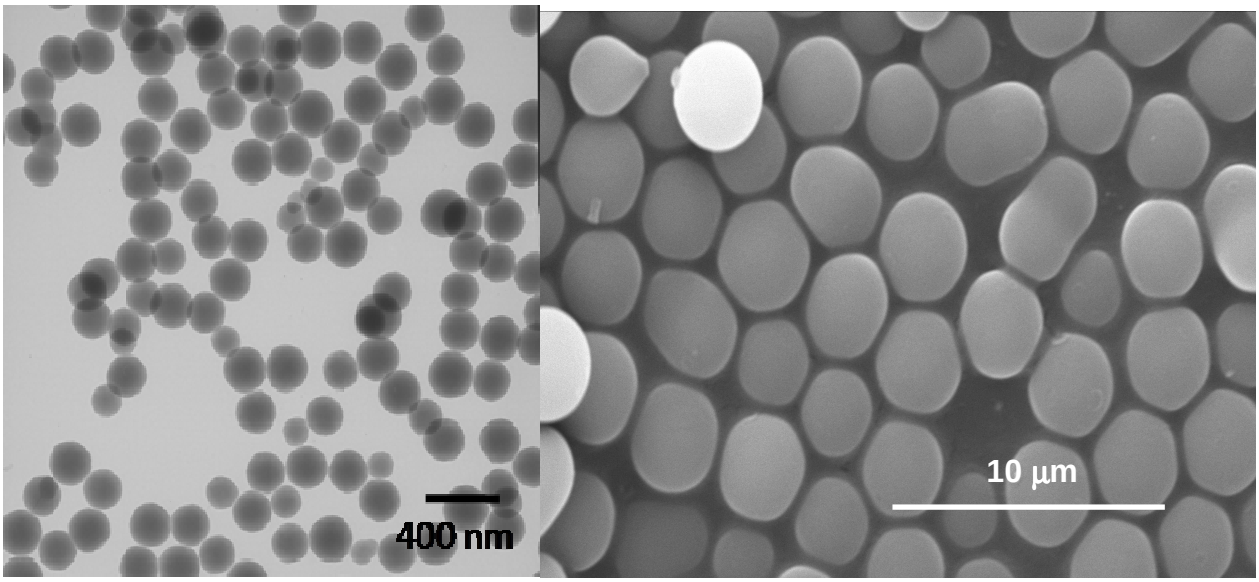

Figure 2. Left: TEM image of sample SiO_2[1], mean diameter size = 204 nm (P = 5 %). Right: SEM image of sample SiO_2[2], mean diameter size = 2.4 microns (P = 30 %).

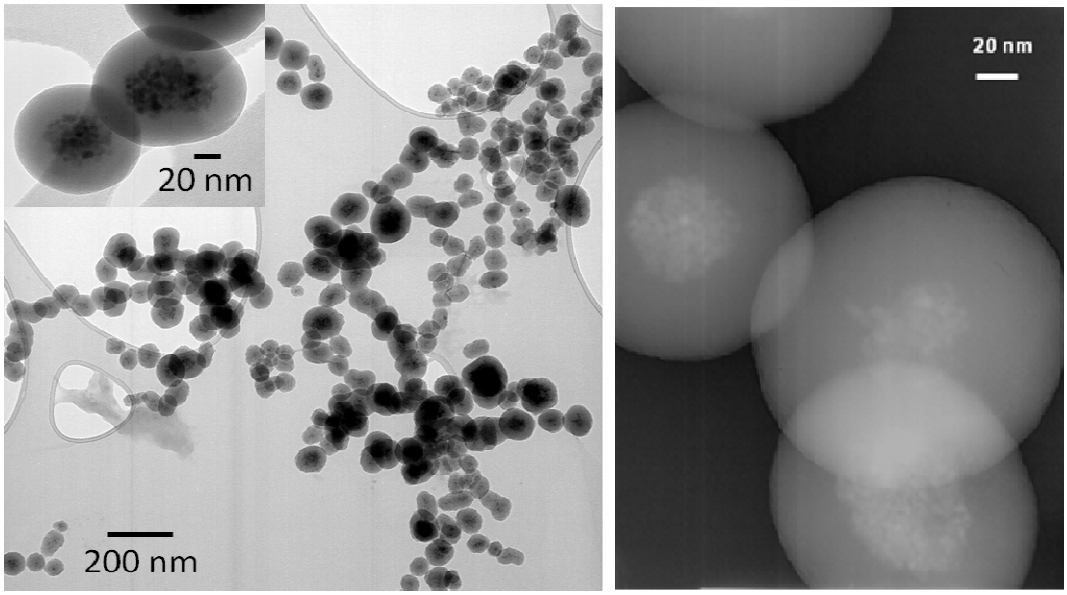

Figure 3. Left TEM image of Fe_2O_3@SiO_2, d=65 nm (P=19%), 9.8 % Fe_2O_3 mass ratio over total mass I . Right TEM image of (Fe_2O_3/QD)@SiO_2, mean diameter=156 (P=19%).

Nitrogen adsorption/desorption isotherms of our systems were measured to obtain qualitative information from the curve shape and quantitative data by applying the BET (Brunauer, Emmet and Teller) and BJH (Barret, Joyner and Halenda) models (for the calculation of the surface area and the pore size, respectively). All the analyzed particles share the type of isotherms, corresponding to type I, which is characteristic of microporous materials. [15] Regarding the surface area, the values are on the lower range of those found for bulk silica aerogels (300-100 m^2/g). As expected from the isotherm shape, micropore area is predominant with a percentage over 75% in most cases. The value of constant C in the BET model equation is negative for almost all the samples, which is attributed, once more, to the presence of micropores. [16] The particles were further studied by infrared spectroscopy (IR) and thermal gravimetric analysis (TGA). Figure 4 shows an IR spectrum of a representative sample. The bands associated to the silica bonds are found at 1052, 959 and 769 cm^{-1}, respectively. Surface hydroxyl groups and adsorbed water are identified at 3400 and 1635 cm^{-1}, respectively. The absence of C-H bands around 3000 cm^{-1} confirms that the organic solvent has been thoroughly extracted, which is a relevant result in view of biomedical applications.

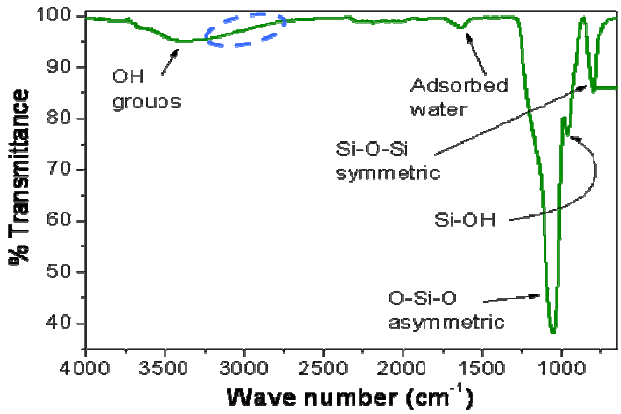

Figure 4. Infrared spectrum of a representative sample. The area encircled in the dashed line highlights the absence of C-H bands.

Thermal gravimetric analysis gives information about the relative mass composition of the sample (see Figure 5). In amorphous silica the surface silicon atoms tend to maintain their tetrahedral coordination with oxygen through the formation of silanol groups or the coordination of oxygen atoms to water molecules. Water is physically adsorbed whereas hydroxyl groups (OH^-) are chemically bonded. The dehydration of silica should be accomplished at 120ºC, although in highly dispersed and porous silica, water is still present at higher temperatures, up to 300ºC. Between 300 and 500ºC the dehydroxylation of the surface takes place: every two vicinal OH^- groups condense into one water molecule and a new siloxane bond (Si-O-Si) is formed. It has been reported that annealing of porous silica above 600ºC is accompanied by sintering, which causes the destruction of the pore structure and consequently an appreciable decrease of the specific surface area. Besides, the isolated hydroxyl groups become closer due to the silica sintering which enables further dehydroxylation of the material. Complete dehydroxylation is only achieved above 1200ºC. The progressive lack of surface hydroxyl groups confers hydrophobicity to the sample. [17] Our porous silica particles have approximately 2.5 ± 0.9 wt.% of physically adsorbed water (below 240ºC), 2.6 ± 0.9 wt.% of water derived from the condensation of vicinal hydroxyl groups (240 to 470ºC) and about 2.9 ± 0.8 wt.% of water derived from the condensation of isolated hydroxyl groups after sintering of silica (over 470ºC) (see Figure 5). The onset of sintering can be identified between 470 and 570ºC by the higher slope in the TGA curve accompanied by the negative peak in the derivative curve. The sample weight tends to stabilize around 92 wt. %, which corresponds to the net mass of silicon and oxygen.

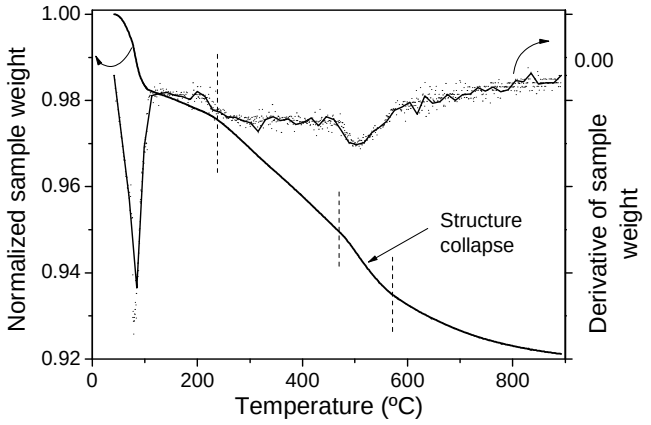

Figure 5. Thermal gravimetric analysis of a representative sample (SiO_2[1] in Ar, 5ºC/min).

The hydroxyl surface coverage can be determined by the TGA analysis. The mass loss over 240ºC corresponds to water molecules derived from the condensation of OH^- groups, not directly to the mass of hydroxyl groups. Then, each desorbed water molecule comes from two hydroxyl groups. The number of hydroxyl groups per surface area is a useful piece of information to plan a synthetic approach for a post-functionalization of the particles. Taking into account the experimental desorbed water and the experimental surface area the OH^- number per surface area unit can be obtained with the following calculation:

$$\mathrm{n^o\,OH^-/nm^2} = \frac{\mathrm{gH_2O}}{\mathrm{100gSiO_2}} \cdot \frac{\mathrm{1molH_2O}}{\mathrm{18gH_2O}} \cdot \frac{\mathrm{2molOH^-}}{\mathrm{1molH_2O}} \cdot 6.022 \cdot 10^{23} \frac{\mathrm{OH^-groups}}{\mathrm{molOH^-}} \cdot \frac{1}{\mathrm{S_{BET}}} \frac{\mathrm{gSiO_2}}{\mathrm{m^2}} \cdot \frac{\mathrm{1m^2}}{\mathrm{10^{18}nm^2}}$$

For sample SiO_2[1]:

$$n^o OH^-/nm^2 = \frac{5.5gH_2O}{100gSiO_2}\cdot\frac{1molH_2O}{18gH_2O}\cdot\frac{2molOH^-}{1molH_2O}\cdot 6.022\cdot 10^{23}\frac{OH^-groups}{molOH^-}\cdot\frac{gSiO_2}{307m^2}\cdot\frac{1m^2}{10^{18}nm^2}$$

$$\boxed{n^o OH^-/nm^2 \approx 12}$$

In the case of core-shell particles, the cores are formed by grouped maghemite and/or quantum dots nanoparticles have diameters between 20 and 60 nm. M(H) curves at 298K for the magnetic materials were measured. They behave as superparamagnets with high magnetization saturation (approx. 60 Am^2/kg Fe_2O_3 at 300K) comparable to the value of the bulk material. These results confirm that there are no strong magnetic dipolar interactions between the particles forming the nucleus and that the supercritical drying has not induced sintering or particle growth. At room temperature, these two situations could induce a magnetic clump in the presence of an external magnetic field which wouldn't be helpful for the biomedical applications targeted since one of the interesting advantages of superparamagnetic particles is that they are only magnetized in the presence of an external magnetic field, avoiding agglomeration and possible embolization of capillary vessels. Zero field cooled- field cooled (ZFC-FC) curves (see Figure 6) confirm the superparamagnetic character of the system. The ZFC presents a well defined narrow peak (indicative of a narrow particle size distribution) and the maximum magnetization value at 60K which corresponds to the blocking temperature. It is worth mentioning that the value of the saturation magnetization (M_s) per kg of Fe_2O_3 for the nanocomposite material is much larger than for the as-synthesized Fe_2O_3 particles (not shown). We believe that it is related to an improvement of the crystallinity of the nanoparticles resulting from the high temperature treatment during the silica shell fabrication.

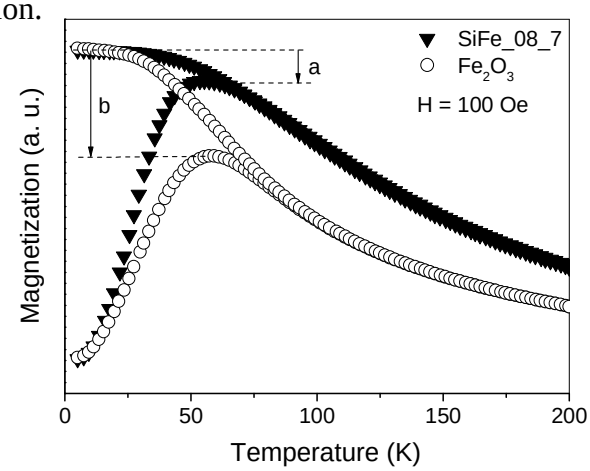

Figure 6. ZFC-FC curves of a representative composite material and its iron oxide nanoparticles counterpart normalized at 5 K, it can be observed that the maximum of the ZFC curve is not shifted to higher temperatures signalling that the particle size has not increased during the silica shell growth.

Experiments of luminescence were carried out to compare the emission intensity in pristine QDs with the one registered for the $(Fe_2O_3/QD)@SiO_2$ system. Typically, a given amount of composite nanoshperes was dispersed in ethanol, while pristine QDs were directly measured in hexane. The wavelength of excitation was fixed at 517 nm. Luminiscence spectrum of QDs shows maximum emission at 600 nm. Luminiscence of $(Fe_2O_3/QD)@SiO_2$ system is very weak (see Fig. 7), quenching of the signal could arise from the proximity of the luminescent QD to the magnetic ones at the cores. [18] However, a weak peak around 630 nm

is noticeable in this sample that does not appear for the purely magnetic system, Fe_2O_3@SiO_2. This involves a red shift attributed to the surface modification of QDs particles during the synthesis process of the composite particles.

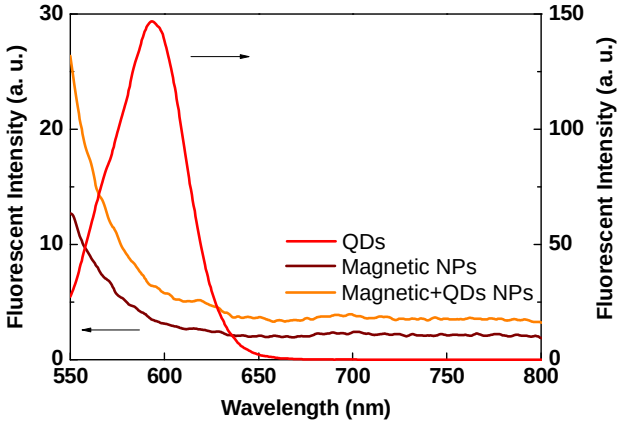

Figure 7. Luminescence spectra of quantum dots dispersed in hexane, magnetic nanoparticles dispersed in ethanol and magnetic and QDs nanoparticles dispersed also in ethanol.

CONCLUSIONS

Silica micro- and nanospheres were synthesized combining sol-gel chemistry and supercritical fluids. This approach reduces the number of steps compared to other sol-gel processing approaches. The particles were obtained as dry and light-weighted powder. Resulting particles were spherical with narrow particle size distributions and tunable sizes ranging from 200 nm to 2 microns. Concerning porosity, all the samples were microporous (d_{pore} < 2 nm). The BET surface areas oscillated between 180 and 320 m^2/g without the use of porogenic agents. No traces of organic residues were detected by IR spectroscopy, what is especially interesting for the biomedical applications. Hydroxyls surface density was determined to be 12 OH^-/nm for the 200 nm system.

In the case of core-shell nanoparticles, the stabilization of the initial sol was achieved by following the reactive addition sequence: acetone-TMOS-water-Fe_2O_3/quantum dots_hexane. Other addition sequence resulted in unstable colloidal dispersions. The core nanoparticles formed clusters in the reactants sol and the cluster size depended on the acetone to hexane volume ratio. Core-shell nanospheres were equally obtained as dry and light powders. The particles were then redispersible in polar solvents, such as water, ethanol and acetone. Core-shell nanospheres were built up of a magnetic and/or QD core surrounded by the silica shell. The shape was spherical and the composite size, which was directly dependent on the core cluster size, ranged from 70 to 200 nm with particle size polydispersity lower than 30%. XRD analyses revealed the presence of amorphous silica and crystalline core. Magnetic or quantum dot nanocrystals do not experience particle growth during the supercritical conditions, neither sintered nor become ferromagnetic. This is an important from the biomedical applications point of view, for instance to avoid embolism for intravenous administration of the nanospheres. The resulting BET surface areas values were lower than those of the silica particles, with values of aprox. 100 m^2/g SiO_2. Composite particles are superparamagnetic at room temperature. The saturation magnetization (M_S) in composite samples almost doubled the one in iron oxide nanoparticles. We attribute the increase of M_S to an improvement of the iron oxide crystallinity due to the silica growing onto its surface at

high temperature. Luminiscence of the composite quantum dot nanospheres is quenched by the proximity of iron oxide nanocrystals.

ACKNOWLEDGEMENTS

The work was partially funded by the Spanish Government (MAT2009-08024 and Consolider-NANOSELEC CSD200700041) and the Generalitat de Catalunya (2009SGR203).

REFERENCES

[1] WILCOX D.L., BERG M., BERNAT T., KELLERMAN D., COCHRAN J.K, in Hollow and Solids Spheres and Microspheres: Science and Technology Associated with their fabrication and applications (Material Research Society Proceedings, Pittsburg), **1995**, p. 372.
[2] STÖBER W. , A. FINK, E. BOHN, J. Colloid Interface Science, Vol. 26, **1968**, p. 62.
[3] LU J., M. LIONG, J. I. ZINK, F. TAMANOI, Small, Vol. 3, **2007**, p. 1341.
[4] LU J., M. LIONG, J. I. ZINK, F. TAMANOI, Advanced Drug Delivery Reviews, Vol. 60, **2008**, p. 1278.
[5] CABAÑAS A., E. ENCISO, C. CARBAJO, M. TORRALVO, C. PANDO, J. RENUNCIO, Chem. Mater., Vol. 17, **2005**, p. 6137.
[6] AYMONIER C., A. LOPPINET-SERANI, H. REVERÓN, Y. GARRABOS, F. CANSELL, J. Supercrit. Fluids, Vol. 38, **2006**, p. 242.
[7] LOY D.A., E. M. RUSSICK, S. A. YAMANAKA, B. M. BAUGHER, Chem. Mater. Vol. 4, **1997**, p. 749.
[8] MONER-GIRONA M., A. ROIG, E. MOLINS, J. LLIBRE, Journal of Sol-Gel Science and Technology, Vol. 26, **2003**, p. 645.
[9] MONER-GIRONA M., A. ROIG, M. BENITO, E. MOLINS, Journal of Materials Chemistry, Vol. 13, **2003**, p. 2066.
[10] TABOADA E., R. SOLANAS, E. RODRÍGUEZ, R. WEISSLEDER, A. ROIG, Avd. Funct. Mater., Vol. 19, **2009**, p. 2319.
[11] CHEN D.X., E. TABOADA, A. ROIG, Journal of Magnetism and Magnetic Materials, Vol. 323, **2011**, p. 2487.
[12] HYEON T., S. S. LEE, J. PARK, Y. CHUNG, H. B. NA, J. Am. Chem. Soc., Vol. 123, **2001**, p. 12798.
[13] HÜSING N. , U. SCHUBERT, Angew. Chem. Int. Ed., Vol. 37, **1998**, p. 22.
[14] When collecting or manipulating the powder, it is advisable to wear a protection mask against particles in order not to inhale the powder which is easily dispersed all over the room. Nevertheless, the toxicity of silica has been widely studied and no signs of systemic toxicity have been observed due to skin or eye contact, inhalation or oral intake.
[15] BRUNAUER S., The adsorption of gases and vapours., Vol I, Physical Adsorption, **1943** Princeton University Press, Princeton.
[16] WEBB P.A., C. ORR, Analytical methods in fine particle technology, **1997**, Micromeritics Instrument Corporation, USA.
[17] UNGER K.K., Porous silica; its properties and use as support in column liquid chromatography, **1979**, Elsevier Scientific Publishing Company, Amsterdam.
[18] HE R., X. YOU, J. SHAO, F. GAO, B. PAN, D. CUI, Nanotech. Vol. 18, **2007**, p. 315601.